Journal of Fisheries
Volume 14 Issue 3 December 2026
Peer Reviewed | Open Access

eISSN 2311-3111
pISSN 2311-729X

DOI: https://doi.org/10.17017/j.fish.1066

Original Article

Alterations in Nile tilapia *Oreochromis niloticus* erythrometry as sensitive indicators of dietary fluoroquinolone antibiotic enrofloxacin toxicity

Ratnapriya Das[1] • Thangapalam Jawahar Abraham[1] • Arya Sen[1] • Prasanna Kumar Patil[2]

[1] *Department of Aquatic Animal Health, West Bengal University of Animal and Fishery Sciences, Kolkata, West Bengal, India*
[2] *Aquatic Animal Health and Environment Division, ICAR-Central Institute of Brackishwater Aquaculture, Chennai, Tamil Nadu, India*

Correspondence
Thangapalam Jawahar Abraham; Department of Aquatic Animal Health, West Bengal University of Animal and Fishery Sciences, Kolkata, West Bengal, India
abrahamtj1@gmail.com

Manuscript history
Received 23 August 2025 | Accepted 15 June 2026 | Published online 18 June 2026

Citation
Das R, Abraham TJ, Sen A, Patil PK (2026) Alterations in Nile tilapia *Oreochromis niloticus* erythrometry as sensitive indicators of dietary fluoroquinolone antibiotic enrofloxacin toxicity. Journal of Fisheries 14(3): 143203. DOI: 10.17017/j.fish.1066

Abstract
The use of antibiotics in aquaculture poses significant health risks to fish and consumers. Adopting and validating a standard, non-lethal, and cost-effective method to monitor fish health is essential. This study investigated the impact of fluoroquinolone antibiotic enrofloxacin (ENF) on the erythrocyte cellular and nuclear morphometric anomalies in *Oreochromis niloticus*. Fish were fed graded doses of ENF at 0 mg, 10 mg, 30 mg, 50 mg and 100 mg kg biomass^{-1} day^{-1} for 15 consecutive days, followed by a 21-day post-dosing observation. The results revealed significant alterations in erythrocyte morphometric characteristics, such as major and minor axes, volume, surface area, cell to nucleus ratio, and surface area to volume ratio due to dietary ENF, indicating its cytotoxicity and perilous effects on fish erythrocytes. The nucleus was shrinking more significantly than the cell under treatment-induced stress. On day 15 of dosing, the surface area to volume ratio increased in the dosing groups, except for the 10× group, which represented an adaptive response in the fish to facilitate greater area for gas exchange to occur. However, the observed dose- and time-dependent erythro-morphometry was reversible once dosing was suspended. The results showed that fish erythrometric abnormalities, a relatively unexplored area of clinical science, can serve as important biomarkers or sensitive indicators of toxicity of veterinary medicinal products in assessing the physiological health status of cultured aquatic organisms.

Keywords: aquaculture; biomarkers; cytotoxicity; fish erythrocytes; medicated feed

1 | INTRODUCTION

The erythrocytes have long captivated biophysicists, cell biologists, and biochemists due to their relatively simple structure and intriguing mechanical and physiological characteristics (Shin *et al*. 2007). Despite extensive research, much remains to be understood about the remarkable resilience of erythrocytes, which undergo significant deformation in the circulatory system but quickly return to their original shape once shear stress is removed (Chien 1987; Bardhan *et al*. 2022). The complexities of blood flow in the cardiovascular system are mainly due to the flow properties of blood and the viscoelastic

properties of blood vessels. Different shear rates at various locations within the cardiovascular system influence the flow properties of blood (Shin *et al*. 2007). The transition from homogeneous flow in large vessels to heterogeneous flow in microvessels is primarily caused by physiological flow conditions and the rearrangement of cellular components, largely dominated by erythrocytes (Stoltz *et al*. 1999). Fish have a closed circulatory system with a heart that pumps blood around the body in a single loop-from the heart to the gills, from the gills to the rest of the body, and then back to the heart (Roberts 2012). The multi-profile flow reduces to a single profile of erythrocytes in capillaries, which are primarily responsible for the exchange of gases and metabolic products, with erythrocyte deformability being a critical factor (Stoltz *et al*. 1999). Erythrocyte deformability, which is primarily determined by internal viscosity, cell morphometry, and shape, enhances flow in microvessels and large arteries at high shear rates (Moriarty and Gibson 2005). Furthermore, toxic substances, such as metal ions, pesticides, anthropogenic aquatic pollutants and pharmaceuticals, are known to induce haemato-pathological changes in fish (Fazio 2019; Witeska *et al*. 2023). Several factors, such as diseases, xenobiotics, veterinary medicinal products (VMPs) and erythrocyte ageing, influence the morphometric parameters in various organisms, including fish (Liu *et al*. 1990; Das *et al*. 2022). Globally, the use of antibiotics has been increasing to control bacterial diseases (Schar *et al*. 2020), but their use harms the physiological and biochemical conditions of fish (Bardhan *et al*. 2022; Abraham *et al*. 2024). Tilapias are the 3rd most farmed fish group after carp and catfish (FAO 2024) and have been reported to consume about 3.4% of the total antibiotics used in aquaculture (Schar *et al*. 2020). According to them, India is the 2nd largest consumer of antibiotics in aquaculture after China and uses the highest quantities of quinolones. Enrofloxacin (ENF) [6-fluoro-7-piperazinyl-4-quinolones], a fluoroquinolone antibiotic, is widely used in veterinary medicine against bacterial infections (Schar *et al*. 2020; Rigos and Kogiannou 2023). The recommended dose of ENF for finfish is 10 mg kg biomass^{-1} day^{-1} for 5 consecutive days (ADCC 2005; CCVP 2020). A perusal of the literature revealed no studies on the impact of antibiotic use on erythro-morphometrical deformities. However, Das *et al*. (2022) documented erythrometric changes in Nile tilapia *Oreochromis niloticus* when fed the dietary antiparasitic drug emamectin benzoate (EB). Antibiotic use is common in Asian aquaculture, where inadequate oversight often leads to excessive dosing (Schar *et al*. 2020). In Indian aquaculture, about 10.14% and 20.29% of carp and catfish farmers, respectively, have reported enrofloxacin applications (Patil *et al*. 2022). Data from target animal safety studies and margin of safety are required for registration of VMPs as per guidelines (FDA 2009). The margin of safety must be determined by testing the drug at higher-than-labelled doses (5 or 10 times the therapeutic dose) for a longer-than-labelled time period (three times the recommended schedule duration) in the target animal species (FDA 2009). Therefore, this experiment assessed the erythro-morphometry of *O. niloticus* as influenced by dietary administration of fluoroquinolone antibiotic enrofloxacin, an unfamiliar area in fish health monitoring, at graded doses of 0 mg, 10 mg, 30 mg, 50 mg and 100 mg kg biomass^{-1} day^{-1} for an extended period of 15 consecutive days, followed by 21-day post-dosing observations under tropical conditions.

2 | METHODOLOGY

2.1 Experimental fish and design

Oreochromis niloticus (15.74±0.80 g and 9.89±0.21 cm) were sourced from a well-maintained, disease-free grow-out farm in Sonarpur, West Bengal, India (22°27′50.215800 N 88°23′07.400400 E). The fish were transported to the laboratory within 3 hours of capture in oxygen-filled double-layered plastic bags. Upon arrival, they were subjected to a 3% saltwater dip and acclimatised for 15 days in 500-L capacity circular fibreglass-reinforced plastic (FRP) tanks, stocked at 50 fish tank^{-1} with continuous aeration. During acclimatisation, they were fed a commercial floating pellet feed (Aquaxcel, Cargill, India), containing 8% fat, 42% protein, 5% fibre, and 11% moisture, thrice daily at 2% bodyweight (BW) in equal portions. After ensuring the fish were infection-free, they were randomly selected from stock tanks and distributed into 15 FRP tanks at 25 fish tank^{-1} for a 7-day pre-dosing acclimatisation period. The fish were then assigned to five groups, viz., Group 1 (0× control, without ENF), Group 2 (1× ENF-dosing [ED] at 10 mg kg biomass^{-1} day^{-1}), Group 3 (3× ED at 30 mg), Group 4 (5× ED at 50 mg), and Group 5 (10× ED at 100 mg), in triplicate. Approximately 50% of the water was replaced every three days to maintain water quality and remove waste. The water quality parameters such as temperature 29.17±2.05°C (morning), 28.57±1.36°C (evening); pH 7.61±0.24; dissolved oxygen 5.74±0.26 mg L^{-1}; ammonia 0.04±0.01 mg L^{-1}; nitrite 0.27±0.02 mg L^{-1}; and nitrate 0.05±0.01 mg L^{-1}] were maintained optimally throughout the experiment.

2.2 Enrofloxacin feed preparation and dose administration

To prepare medicated feeds, the inclusion rate for pure ENF powder (Sigma-Aldrich, India; CAS No: 93106-60-6; Product Number: 17849-25G-F) was calculated to provide five graded doses, viz., 0 mg, 10 mg, 30 mg, 50 mg, and 100 mg kg biomass^{-1} day^{-1} for 15 consecutive days. The process of adding ENF to the basal feed pellet by employing vegetable oil as a binder was previously described. The control feed was top-coated similarly, only with vege-

table oil (Das *et al*. 2024). The study duration was 43 days, consisting of a 7-day acclimation, 15 days of ED, and 21 days post-ENF-dosing (PED). The fish were fed a control feed during the pre-dosing and post-dosing periods. Throughout the 15-day dosing, the ENF feeds were given to the respective groups thrice daily at 2% BW in equal portions. Daily observations included feeding behaviour, mortality, and the quantification of uneaten feed left in the tank one hour after each feeding (Bardhan *et al*. 2022).

2.3 Blood collection, smear preparation and erythrometric analysis

Blood sampling was conducted on days 0 and 15 of ED and day 21 PED, as described previously (Das *et al*. 2022, 2024). In brief, three fish from each tank were anaesthetised with clove oil (40 µL L^{-1}), and blood was collected via caudal vein puncture (Roberts 2012). Immediately, a drop of blood, without an anticoagulant, was placed on a microscope slide and smeared. The blood smear slides were stained with 5% Giemsa, air-dried, and examined under a microscope (Olympus, Japan, Model: BX51) equipped with an SCO-LUX 16 MP camera, using the oil immersion lens (Das *et al*. 2022). Image capture and processing were performed with ToupTek ToupView software (Version x64, 4.11). The major parameters measured for erythrocytes and their nuclei included the major axis, minor axis, volume, and surface area. A total of 50 randomly selected, undamaged, nearly oval-shaped erythrocytes from 12 smears per treatment tank were measured (Das *et al*. 2022). The measurements from all 50 erythrocytes within each tank were averaged to yield a single tank mean for each erythrocyte parameter, which served as the experimental unit in subsequent statistical analyses. Since tilapia erythrocytes exhibit an ellipsoidal shape, their volume was calculated using the formula $V = (4/3)\pi AB^2$, where 'A' and 'B' represent the major and minor semi-axes of the cell, respectively (Uzunova 2002). The surface area of the erythrocytes and nuclei was calculated using $S = (ab\pi)/4$, where 'a' and 'b' denote the major and minor axes of the erythrocytes and nuclei, respectively (Dorafshan *et al*. 2008).

2.4 Erythrocyte cell to nucleus (C/N), and surface area to volume ratio

The erythrocyte cell to nucleus (C/N) ratio was determined for the major axis, minor axis, volume, and surface area of the erythrocytes. For each parameter, the ratio was calculated as below.

Larger axis ratio = Larger axis of erythrocyte / Larger axis of nucleus

Minor axis ratio = Minor axis of erythrocyte / Minor axis of nucleus

Volume ratio = Volume of erythrocyte / Volume of nucleus

Surface area ratio = Surface area of erythrocyte / Surface area of nucleus

The erythrocyte surface area to volume ratio was calculated by dividing the surface area of the erythrocyte by the volume of the erythrocyte.

2.5 Statistical analysis

For each erythrocyte parameter, the mean value of 50 cells measured per tank was calculated, and these tank means (n = 3 tanks per treatment group) were used as the experimental unit to avoid pseudo-replication. Before analysis, the normality of data distribution within each group was assessed using the Shapiro-Wilk test, and homogeneity of variance across groups was evaluated using Levene's test. Both assumptions were satisfied for all parameters ($p > 0.05$). The tank means, expressed as mean ± standard deviation of three replicate tanks, were analysed by one-way ANOVA. The significance of differences at $p < 0.05$ among treatment groups and sampling timepoints was confirmed using the Tukey post-hoc test for pairwise comparison of means. All statistical analyses were conducted using the Statistical Package for the Social Sciences (IBM-SPSS), version 23.0.

3 | RESULTS

Compared to the control (Figure 1A), the major axis length of the erythrocytes significantly decreased [$F_{(4,10)}$ = 18.64, $p < 0.05$] from the initial level in a dose-dependent manner in 15 days of ED (Figure 1B–1E). Following the dose cessation, the major axis began to return to normalcy in the 1× and 3× groups, while the 5× and 10× groups had significantly diminished major axis [$F_{(4,10)}$ = 8.12, $p < 0.05$]. The minor axis length of the erythrocytes reduced only slightly from the initial level in the ED groups, except for the 10× group, which decreased significantly [$F_{(4,10)}$ = 4.89, $p < 0.05$]. However, the minor axis nearly returned to normal on day 21 PED. The erythrocyte volume was reduced by 6.4% in the 1× group and significantly by 30% in the 10× group [$F_{(4,10)}$ = 14.23, $p < 0.05$] compared to the control. Though the erythrocyte volume began to normalise in all groups following the dose cessation, the reduction persisted except for the 1× group. The surface area of the erythrocytes reduced significantly [$F_{(4, 10)}$ = 11.56, $p < 0.05$] on day 15 of ED than in the control. However, the differences in surface area among the 3×-10× groups were insignificant [$F_{(4, 10)}$ = 1.68, $p > 0.05$]. Upon dose suspension, the erythrocyte surface area began to return to normal. In the 1× group, the major axis length of the erythrocyte nucleus had insignificant changes on day 15 of ED [$F_{(4,10)}$ = 2.01, $p > 0.05$] compared to the control. However, in other groups, it decreased significantly and dose-dependently [$F_{(4,10)}$ = 22.15, $p < 0.05$]. With the dose cessation, the major axis started to normalise in the lower dose groups, while the 5× and 10× groups continued to show significantly shorter lengths [$F_{(4,10)}$ = 13.78, $p < 0.05$].

A slight reduction in minor axis length from the initial level was noted in the lower dose groups, while the 5× and 10× groups experienced a significant decrease [$F_{(4,10)}$ = 6.92, $p < 0.05$]. Nonetheless, the minor axis length of all groups increased toward normalcy over time. The nuclear volume of the 1× and 3× groups reduced insignificantly [$F_{(4,10)}$ = 1.54, $p > 0.05$] from the initial level, while the reduction was significant [$F_{(4,10)}$ = 10.54, $p < 0.05$] in the 5× and 10× groups, with the maximum in the 10× group. Though the nuclear volume began to normalise in all groups with dose cessation, the reduction persisted in the 5× and 10× groups. The surface area of the nucleus was reduced significantly in the ED groups [$F_{(4,10)}$ = 16.42, $p < 0.05$] compared to the control. The reduction was the least in the 1× group. Upon dose suspension, the nuclear surface area returned to normal (Table 1). The formation of micronuclei was also noted in all ED groups. The erythrocyte C/N ratio exhibited dose-dependent changes for the measured parameters (Figure 2). Significant increases were observed in larger and minor axes, and surface area in overdosed (3×, 5× and 10×) groups on day 15 of ED [$F_{(4,10)}$ = 25.81, $p < 0.05$], with the 10× group showing the greatest alterations. Although a slight decline was noted on day 21 of PED, the anomalies persisted. On day 15, the surface area to volume ratio was increased in the ED groups, except for the 10× group, which reduced slightly. Post-dosing, compared to the control and 1× groups, the extent of increment in surface area to volume ratio was greater in the 3× group, followed by the 5× and 10× groups (Figure 3). The day- and dose-specific percentage reduction in all the parameters compared to control values are documented in supplementary Table 1.

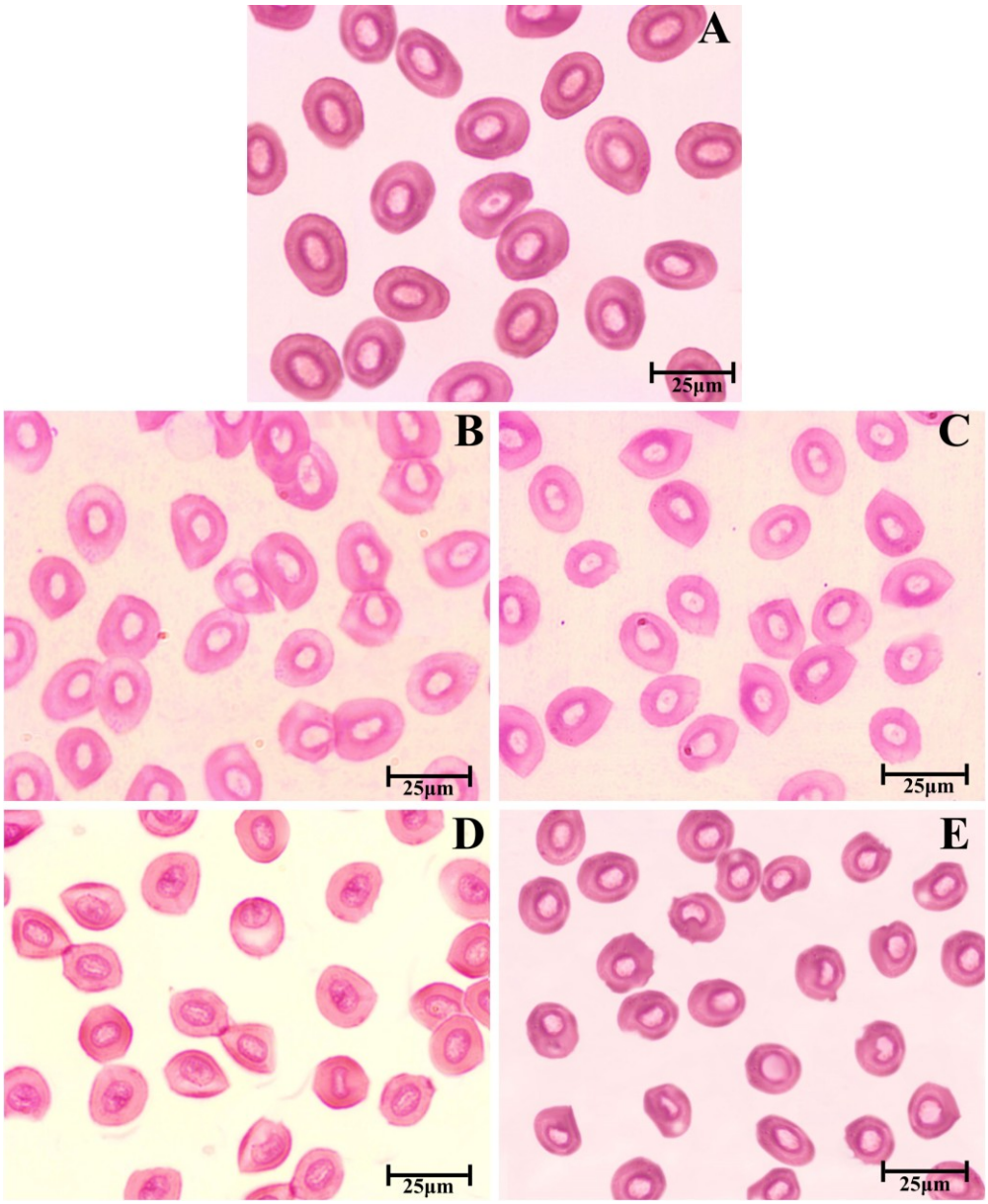

FIGURE 1 Photomicrographs showing dose-dependent morphological variations in the erythrocytes of *Oreochromis niloticus* fed graded doses of enrofloxacin for 15 consecutive days. [A] Control group, [B] 1× group at 10 mg, [C] 3× group at 30 mg, [D] 5× group at 50 mg and [E] 10× group at 100 mg kg biomass^{-1} day^{-1}, ×1,000 Giemsa staining.

TABLE 1 Erythrocyte morphometry of *Oreochromis niloticus* fed dietary enrofloxacin (ENF) at 0, 10, 30, 50, and 100 mg kg biomass^{-1} day^{-1} for 15 consecutive days and observed for day 21 post-dosing.

Dose	Erythrocyte			Nucleus		
	Day 0	Day 15 ED	Day 21 PED	Day 0	Day 15 ED	Day 21 PED
Larger axes (µm)						
0×	20.11-22.24 (21.67±0.25)^{1a}	20.27-23.56 (21.98±0.71)^{1a}	20.56-23.67 (22.04±0.98)^{1a}	8.18-9.36 (9.15±0.31)^{1a}	8.11-10.09 (9.21±0.15)^{1a}	8.12-10.22 (9.25±0.26)^{1a}
1×	20.19-22.16 (22.03±0.37)^{1a}	19.18-22.09 (20.86±0.88)^{2b}	20.33-22.36 (22.11±0.75)^{1a}	8.12-9.57 (9.35±0.58)^{1a}	8.02-10.67 (9.11±0.81)^{1a}	8.21-9.67 (9.20±0.21)^{1a}
3×	20.36-22.73 (21.98±0.57)^{1a}	19.00-21.58 (20.78±0.89)^{2b}	20.45-23.04 (21.99±0.06)^{1a}	8.45-9.89 (9.05±0.36)^{1a}	7.89-9.77 (8.67±0.56)^{1,2a}	8.89-9.92 (8.76±0.42)^{1,2a}
5×	20.24-22.46 (21.87±0.91)^{1a}	18.57-21.09 (19.54±0.89)^{3b}	19.87-21.08 (20.18±0.14)^{2b}	8.87-9.89 (9.17±0.55)^{1a}	7.34-9.66 (8.56±0.39)^{2b}	8.26-9.27 (8.54±0.92)^{2,3b}
10×	20.21-22.41 (21.77±0.91)^{1a}	18.01-20.57 (19.09±0.23)^{3b}	19.15-20.97 (19.99±0.35)^{2c}	8.25-9.39 (9.24±0.87)^{1a}	6.73-8.11 (7.04±0.88)^{3b}	7.34-9.66 (8.09±0.39)^{3c}
Minor axes (µm)						
0×	15.30-16.34 (15.99±0.39)^{1a}	15.13-16.05 (15.87±0.13)^{1a}	15.41-16.12 (15.71±0.16)^{1a}	5.37-7.48 (6.27±0.47)^{1a}	5.59-7.89 (6.49±0.77)^{1a}	5.27-7.81 (6.57±0.42)^{1a}
1×	15.19-16.77 (16.13±0.66)^{1a}	15.24-16.28 (15.17±0.88)^{1b}	15.13-16.76 (15.68±0.13)^{1a}	5.47-7.98 (6.38±0.97)^{1a}	5.07-7.76 (5.87±0.48)^{2a}	5.13-7.37 (6.17±0.87)^{1,2a}
3×	15.37-16.89 (16.04±0.31)^{1a}	15.09-16.11 (15.12±0.16)^{1b}	15.21-16.62 (15.49±0.23)^{1a,b}	5.13-8.32 (6.52±0.32)^{1a}	4.87-6.81 (5.36±0.16)^{2,3b}	5.37-7.48 (5.98±0.21)^{2c}
5×	15.25-16.79 (16.11±0.91)^{1a}	14.38-16.09 (14.98±0.23)^{1,2b}	15.78-16.79 (15.28±0.23)^{1b}	6.34-7.94 (6.29±0.37)^{1a}	4.11-6.23 (5.12±0.88)^{3b}	5.34-6.89 (5.67±0.17)^{2,3c}
10×	15.37-16.89 (16.09±0.51)^{1a}	14.21-15.87 (14.23±0.26)^{2b}	14.88-15.79 (14.76±0.21)^{1b}	6.47-8.01 (6.78±0.65)^{1a}	4.09-5.79 (5.01±0.65)^{3b}	5.11-6.45 (5.32±0.42)^{3b}
Volume (µm^3)						
0×	2465.47-3075.24 (2978.86±12.57)^{1a}	2503.37-3109.85 (2934.76±19.45)^{1a}	2472.83-3445.67 (2912.54±19.23)^{1a}	142.45-324.28 (225.17±8.15)^{1a}	142.99-325.13 (220.16±6.68)^{1a}	136.57-341.25 (222.73±9.36)^{1a}
1×	2434.87-3131.90 (2918.56±9.99)^{1a}	2234.80-3002.32 (2731.66±18.16)^{2b}	2371.47-3105.06 (2898.51±17.09)^{1a}	140.35-330.19 (235.25±7.98)^{1a}	138.08-312.34 (214.65±4.98)^{1b}	139.34-324.67 (218.17±7.45)^{1b}
3×	2458.44-3120.96 (2934.71±19.12)^{1a}	2154.94-2850.53 (2605.33±15.39)^{3b}	2312.16-3045.51 (2754.84±13.09)^{2c}	144.36-331.36 (231.45±8.96)^{1a}	125.46-279.65 (205.39±7.41)^{1b}	130.08-309.24 (216.62±7.99)^{1a,b}
5×	2439.16-3110.28 (2956.38±6.98)^{1a}	2009.54-2774.47 (2403.58±11.39)^{4b}	2150.27-2941.24 (2509.51±11.09)^{3c}	146.38-335.58 (224.78±10.02)^{1a}	116.76-249.17 (159.67±6.03)^{2b}	125.63-236.59 (179.64±9.04)^{2c}
10×	2437.54-3105.14 (2987.55±16.98)^{1a}	1991.42-2547.44 (2107.28±8.39)^{5b}	2088.58-2717.24 (2307.18±19.39)^{4c}	145.02-355.53 (228.38±8.99)^{1a}	109.59-221.44 (136.72±6.08)^{3b}	121.18-229.87 (159.98±7.90)^{3c}
Surface area (µm^2)						
0×	243.56-312.58 (259.15±8.07)^{1a}	241.25-315.78 (262.10±7.89)^{1a}	246.38-314.28 (252.14±5.89)^{1a}	29.88-66.58 (45.87±6.87)^{1a}	31.69-63.55 (49.04±6.58)^{1a}	29.58-60.25 (45.98±5.89)^{1a}
1×	250.73-313.35 (261.16±9.67)^{1a}	230.14-268.19 (248.66±9.51)^{1a}	242.74-289.33 (257.28±6.15)^{1a}	27.17-63.29 (50.12±8.71)^{1a}	27.99-59.49 (42.65±5.13)^{1b}	30.49-64.99 (46.33±7.71)^{1a,b}
3×	245.35-302.12 (261.38±5.36)^{1a}	217.34-232.36 (225.26±6.98)^{2b}	223.36-254.20 (237.74±5.23)^{2b}	28.87-65.77 (51.31±5.89)^{1a}	25.45-52.19 (41.37±7.05)^{2b}	27.99-61.23 (39.96±8.11)^{1,2b}
5×	251.39-316.58 (264.12±7.67)^{1a}	209.34-211.14 (216.12±7.92)^{2b}	215.57-231.24 (227.23±7.23)^{2b}	29.39-64.29 (49.39±8.89)^{1a}	24.89-49.76 (34.76±8.17)^{3b}	26.74-56.44 (39.17±5.25)^{2b}
10×	255.58-314.25 (261.25±9.17)^{1a}	211.25-247.11 (201.14±9.12)^{3b}	214.99-261.24 (232.25±8.99)^{2c}	25.39-64.29 (52.36±6.68)^{1a}	21.07-41.75 (30.72±4.86)^{3b}	21.98-50.21 (35.54±7.09)^{2b}

a–c: Values sharing uncommon alphabets within the row for each parameter and dose differed significantly ($p < 0.05$). 1–5: Values sharing uncommon numerals within the column for each parameter differed significantly ($p < 0.05$). ED: ENF-dosing and PED: post-ENF-dosing.

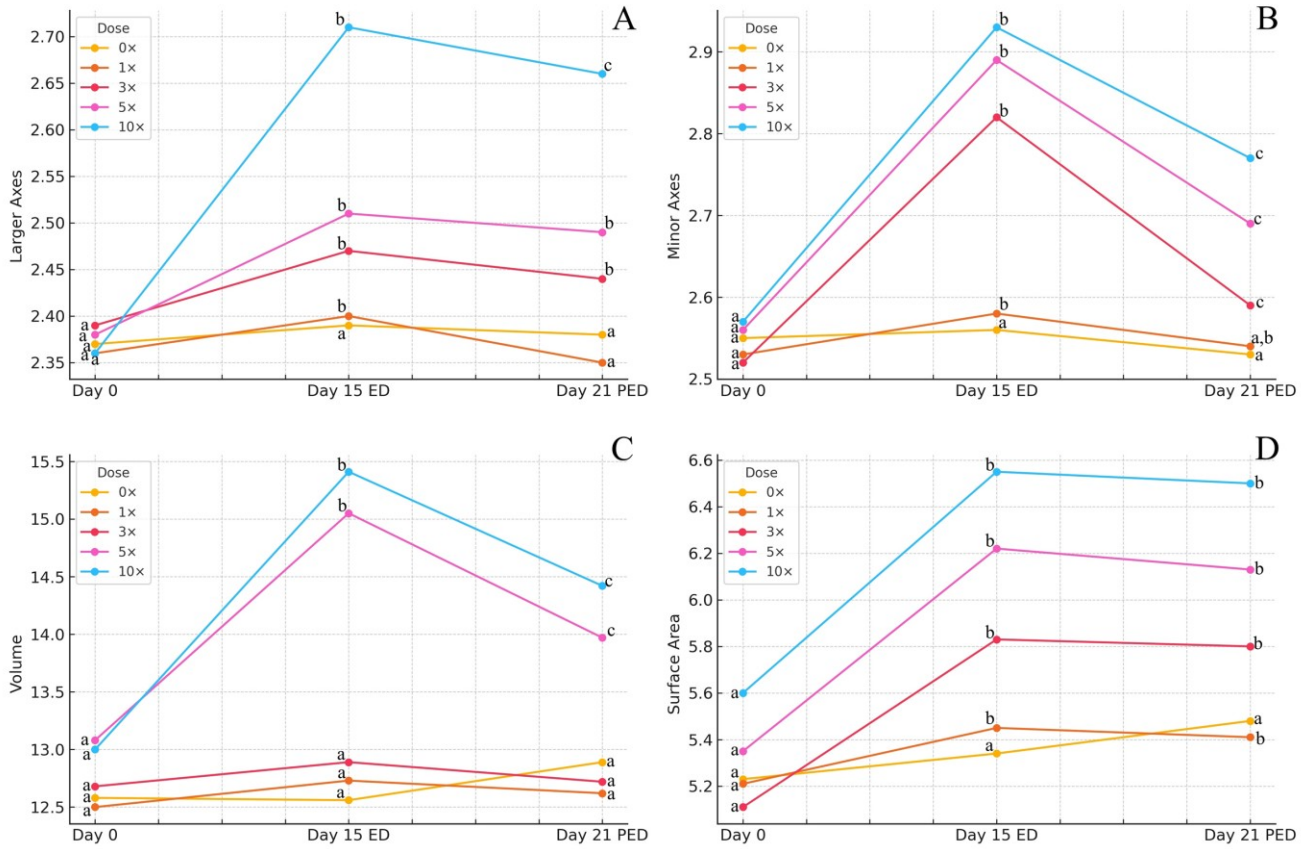

FIGURE 2 Variations in erythrocyte cell to nucleus (C/N) ratio in *Oreochromis niloticus* fed dietary enrofloxacin (ENF) at 0, 10, 30, 50, and 100 mg kg biomass^{-1} day^{-1} for 15 consecutive days and observed for 21 days post-dosing. [A] Larger axes, [B] Minor axes, [C] Volume, and [D] Surface area. a-c: Values sharing uncommon alphabets for a particular dose at different time-points differed significantly ($p < 0.05$).

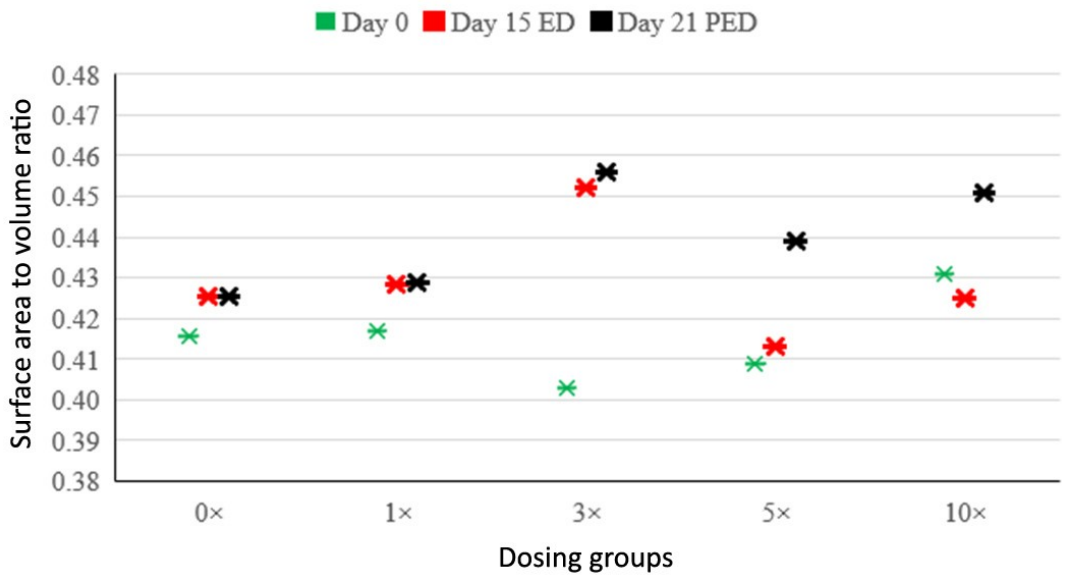

FIGURE 3 Variations in erythrocyte surface area to volume ratio in *Oreochromis niloticus* fed dietary enrofloxacin (ENF) at 0, 10, 30, 50, and 100 mg kg biomass^{-1} day^{-1} for 15 consecutive days and observed for 21 days post-dosing. ED: Enrofloxacin dosing; PED: Post-enrofloxacin dosing.

4 | DISCUSSION

As erythrocytes adjust to a higher volume with a comparatively lower surface area, they deform uniaxially to fit the available space, maintaining their volume and surface area under normal physiological conditions (Shin *et al*. 2007). The measurements of the control erythrocytes and the nuclei of *O. niloticus* were consistent with earlier observations (Das *et al*. 2022). ENF has been reported to induce oxidative stress in fish (Wang *et al*. 2009; Sehonova *et al*. 2019; Shi *et al*. 2023), and such oxidative stress has been shown to cause protein misfolding and the unfolded protein response, potentially leading to erythrocyte shape changes (Chico *et al*. 2018). In our previous study, ENF administration led to dose- and time-dependent variations in haematology and haematological indices (Das *et al*. 2024). Although direct measures of oxidative stress were not assessed in the present study, the observed erythrocyte shape changes may, at least in part, be attributable to ENF-induced oxidative stress, which could compromise cell structural integrity and membrane stability. Our previous study confirmed several erythrocyte morphological changes like membrane crenation, cytoplasmic vacuolations, elongation, teardrop shapes, and other abnormal shapes, and nuclear alterations like notched, blebbed, bilobed, micronuclei, and peripheral nuclei upon prolonged and excessive ENF-dosing (Das *et al*. 2024). The presence of micronuclei in the ED groups is consistent with a possible genotoxic effect of ENF, as micronucleus formation is a widely used indicator of chromosomal instability and DNA strand breakage (Fenech 2000). However, direct DNA damage was not quantified in the present study, and this interpretation should be considered inferential. If genotoxic injury did occur, it could potentially contribute to the observed reduction in nuclear volume by reducing the amount of intact genetic material housed within the nucleus. Alternatively, karyolysis, the dissolution of nuclear structure through enzymatic chromatin degradation, may also represent another plausible mechanism underlying the observed nuclear volume reduction. Yet, this requires confirmation through dedicated cytochemical or molecular analyses. As the nuclear material breaks down, the nucleus loses its defined shape and structure, leading to a volume reduction.

The erythrocyte morphology of certain healthy freshwater fish species was documented (Najiah *et al*. 2008). However, no reports are available on the impact of widespread antibiotic use in aquaculture on the erythrometric deformities for comparison. Our earlier reports documented a decrease in all erythrometric parameters in *O. niloticus* upon dietary EB administration for 7 days (Das *et al*. 2022). The erythrometric deformities have also been demonstrated in several organisms under varied conditions, such as zebrafish *Danio rerio* exposed to microplastics (da Costa Araújo *et al*. 2020), chicken *Gallus gallus domesticus* treated with ZnO nanoparticles (Vieira *et al*. 2019), marsh frog *Pelophylax ridibundus* exposed to heavy metals polluted environments (Zhelev *et al*. 2017) and *Lacerta agilis* subjected to anthropogenic disturbance (Drobot and Remizova 2012). Conversely, Tomova *et al*. (2009) observed an increase in erythrocyte diameter and surface area of Prussian carp *Carassius gibelio* exposed to $ZnSO_4 \cdot 7H_2O$. Upon ED suspension, the erythrometric deformities began to recover, demonstrating tilapia's adaptability, ability to overcome the stress induced by graded doses and tolerance to ENF. Several earlier studies reported stress-induced erythrocyte and nuclear abnormalities in *Channa punctatus* (Sawhney and Johal 2000), *Cirrhinus mrigala* (Bhatnagar *et al*. 2016), *Barbonymus gonionotus* (Sadiqul *et al*. 2017), *D. rerio* (Shahjahan *et al*. 2019), and *O. niloticus* (Majumder and Kaviraj 2019; Al-Emran *et al*. 2022), following exposure to several organophosphate pesticides. As the erythrocytes are primarily involved in the exchange of gases and metabolic wastes, their morphometric changes can, therefore, serve as reliable indicators of the pathophysiological status of fish.

The rise in C/N ratio of all measured parameters, despite concurrent reductions in the absolute dimensions of both the cell and nucleus, demonstrated that the nucleus shrank proportionally more than the cell under ENF-induced stress, a pattern directly supported by the morphometry of the present study. This disproportionate nuclear reduction is consistent with patterns of nuclear damage or condensation reported in association with cytotoxic and genotoxic conditions in aquatic species (Çavaş and Ergene-Gözükara 2005), though these specific mechanisms were not directly assessed here. The morphological profile observed a more condensed nucleus relative to cell size, bearing resemblance to nuclear pyknosis, a morphological hallmark associated with early apoptosis in the broader literature (Fenech 2000). However, confirming this interpretation would require dedicated cytological assays and nuclear staining, or caspase activity measurements, which were beyond the scope of the present study. Our findings suggested that the nucleus may be comparatively more vulnerable to pharmaceutical-induced stress than the cytoplasm, an observation that warrants further mechanistic investigation. Comparable morphological patterns were reported by Hemalatha *et al*. (2019), who observed nuclear shrinkage in fish erythrocytes exposed to triclosan and associated this with chromatin condensation and disruption of mitosis, lending contextual support to the present observations. The elevated C/N ratio in the overdosed groups may additionally reflect a shift in cellular resource allocation favouring cytoplasmic maintenance over nuclear integrity under conditions of persistent chemical stress, though this remains hypothetical, pending direct mechanistic confirmation. The surface area of the recommended dose group at the end of the experiment was higher than on day 0, indi-

cating persistent ENF-induced stress on fish erythrocytes and accrual of residues in the kidneys, as confirmed in our earlier research (Das *et al*. 2024). Besides, the dose- and time-dependent variations in surface area to volume ratio represented an adaptive response of fish to facilitate a greater area for gas exchange to occur, enhancing the efficiency of the gas exchange process. Nevertheless, the degree of surface area to volume ratio increment was comparatively higher in the 3× group, possibly due to the ability of this group to adapt to the changing environment induced by ED better than the 5× and 10× groups, and the reduced metabolic needs of damaged erythrocytes in the overdosed groups. These morphometric shifts could serve as sensitive indicators of early-stage, sub-lethal toxicity of VMPs in fish. The sustained elevation of C/N ratios in overdosed groups during the post-dosing period suggested that nuclear recovery is either delayed or incomplete, even if some systemic compensation occurs.

5 | CONCLUSIONS

Fish farmers often abuse antibiotics due to a lack of awareness, ease of access, and pressure to prevent disease losses quickly. Limited regulation and veterinary support further encourage misuse, leading to risks like antibiotic resistance and environmental harm. The results of the present study indicated that dietary ENF administration can result in significant alterations in the erythrometry of *O. niloticus*. The overdose and prolonged dose of ENF were found to be toxic to fish erythrocytes and their functions. The surface area-to-volume ratio increments in the dosing groups indicated an adaptive response in the fish, allowing for a larger area for gas exchange to occur. The reversibility of the measured erythrometric changes after dose discontinuation highlighted the fish's ability to tolerate and adapt to the overdoses. Further, the erythrometric alterations can serve as vital indicators of the harmful effects of VMPs on cultured fish, as this approach is non-lethal and cost-effective. Overall, this study identified ENF as a stressor capable of causing cytotoxicity, which is noteworthy while planning for the treatment or prevention of diseases in aquaculture. Despite the limited research on erythrometric changes in fish, further studies in this area would provide valuable insights into the pathophysiological conditions. Future studies examining the impact of various antibiotics or stressor combinations may yield insightful information and more precise references to increase our understanding of these medications' potential negative side effects on fish health. Besides, aquaculture farmers are responsible and adhere to the regulatory protocols for antibiotic usage to ensure sustainability.

ACKNOWLEDGEMENTS

The authors thank the Vice-Chancellor, West Bengal University of Animal and Fishery Sciences, Kolkata, for providing the necessary facilities for this work. This work was supported by the Indian Council of Agricultural Research (ICAR), Government of India, New Delhi, under the All-India Network Project on Fish Health (Grant F.No. CIBA/AINP-FH/2015-16 dated 02.06.2015).

ETHICAL APPROVAL

The experimental protocols were approved by the ICAR, New Delhi, under the All-India Network Project on Fish Health (F.No. CIBA/AINP-FH/2015-16 dated 16.7.2015) as per the guiding principles of the Committee for the Purpose of Control and Supervision of Experiments on Animals (CPCSEA), Government of India.

CONFLICT OF INTEREST

The author declares no conflict of interest.

AUTHORS' CONTRIBUTION

Ratnapriya Das and Arya Sen: Investigation, formal analysis, data curation, software, writing-original draft; Thangapalam Jawahar Abraham: Conceptualisation, methodology, project administration, supervision, writing-reviewing and editing; Prasanna Kumar Patil: Conceptualisation, methodology and funding acquisition. All authors agreed with the results and conclusions.

DATA AVAILABILITY STATEMENT

The data supporting this study's findings are available on request from the corresponding author.

REFERENCES

Abraham TJ, Patel JB, Bardhan A, Rajisha R, Panda SK, Patil PK (2024) Safety, tolerability and biological responses of *Oreochromis niloticus* juveniles upon oral oxolinic acid administration. Journal of Veterinary Pharmacology and Therapeutics 47(2): 121–133.

ADCC (2005) Handbook of Fishery Drugs. Agriculture Department Compiling Committee, China Agriculture Press, Beijing.

Al-Emran M, Hasan NA, Khan MP, Islam SMM, Bashar A, … Sumon KA (2022) Alterations in hematological parameters and the structure of peripheral erythrocytes in Nile tilapia (*Oreochromis niloticus*) exposed to profenofos. Environmental Science and Pollution Research 29(19): 29049–29061.

Bardhan A, Abraham TJ, Singha J, Sar TK, Rajisha R, … Patil PK (2022) Histopathological aberrations and oxidative stress responses in Nile tilapia *Oreochromis niloticus* as influenced by dietary florfenicol and its metabolites. Aquaculture 559: 738447.

Bhatnagar A, Yadav AS, Cheema N (2016) Genotoxic effects of chlorpyrifos in freshwater fish *Cirrhinus mrigala* using micronucleus assay. Advanced Biology 2016(1): 9276963.

Çavaş T, Ergene-Gözükara S (2005) Induction of micronu-

clei and nuclear abnormalities in *Oreochromis niloticus* following exposure to petroleum refinery and chromium processing plant effluents. Aquatic Toxicology 74(3): 264–271.

CCVP (2020) ENF powder (for aquaculture application). Commission of Chinese Veterinary Pharmacopoeia. http://124.126.15.169:8081/cx/#. Accessed 10 September 2023.

Chico V, Puente-Marin S, Nombela I, Ciordia S, Mena MC, … Ortega-Villaizan MDM (2018) Shape-shifted red blood cells: a novel red blood cell stage? Cells 7(4): 31.

Chien S (1987) Red cell deformability and its relevance to blood flow. Annual Review of Physiology 49(1): 177–192.

da Costa Araújo AP, de Andrade Vieira JE, Malafaia G (2020) Toxicity and trophic transfer of polyethylene microplastics from *Poecilia reticulata* to *Danio rerio*. Science of the Total Environment 742: 140217.

Das R, Abraham TJ, Sen A, Rajisha R, Nadella RK, … Patil PK (2024) Impact of graded doses of enrofloxacin on the safety and biological responses of Nile tilapia *Oreochromis niloticus*. Drug and Chemical Toxicology 48(4): 784–796.

Das R, Abraham TJ, Singha J, Bardhan A, Patil PK (2022) Dietary emamectin benzoate induces dose-dependent variations in haemato-biochemical and erythrocyte-metric parameters of *Oreochromis niloticus* (L.). Aquaculture 561(2): 738680.

Dorafshan S, Kalbassi MR, Pourkazemi M, Amiri BM, Karimi SS (2008) Effects of triploidy on the Caspian salmon *Salmo trutta caspius* haematology. Fish Physiology and Biochemistry 34(3): 195–200.

Drobot GP, Remizova OS (2012) Using the hematological parameters of *Lacerta agilis* L. for estimating the anthropogenically disturbed territories. Proceedings of the Samara Scientific Center of the Russian Academy of Sciences 14(8): 1887–1890.

FAO (2024) The State of World Fisheries and Aquaculture 2024, Blue Transformation in Action. Food and Agriculture Organization, Rome.

Fazio F (2019) Fish hematology analysis as an important tool of aquaculture: a review. Aquaculture 500: 237–242.

FDA (2009) Target Animal Safety for Veterinary Pharmaceutical Products VICH GL43. Adopted at Step 7 of the VICH Process by the VICH Steering Committee in July 2008 for implementation in July 2009. Food and Drug Administration. Center for Veterinary Medicine, United States Department of Health and Human Services, 19p.

Fenech M (2000) The in vitro micronucleus technique. Mutation Research - Fundamental and Molecular Mechanisms of Mutagenesis 455(1–2): 81–95.

Hemalatha D, Nataraj B, Rangasamy B, Shobana C, Ramesh M (2019) DNA damage and physiological responses in an Indian major carp, *Labeo rohita*, exposed to an antimicrobial agent, triclosan. Fish Physiology and Biochemistry 45(4): 1463–1484.

Liu SC, Derick LH, Agre P, Palek J (1990) Alteration of the erythrocyte membrane skeletal ultrastructure in hereditary spherocytosis, hereditary elliptocytosis, and pyropoikilocytosis. Blood 76(1): 198–205.

Majumder R, Kaviraj A (2019) Acute and sublethal effects of organophosphate insecticide chlorpyrifos on freshwater fish *Oreochromis niloticus*. Drug and Chemical Toxicology 42(5): 487–495.

Moriarty PM, Gibson CA (2005) Association between hematological parameters and high-density lipoprotein cholesterol. Current Opinion in Cardiology 20(4): 318–323.

Najiah M, Nadirah M, Marina H, Lee SW, Nazaha WH (2008) Quantitative comparisons of erythrocyte morphology in healthy freshwater fish species from Malaysia. Research Journal of Fisheries and Hydrobiology 3(1): 32–35.

Patil PK, Mishra SS, Pradhan PK, Manna SK, Abraham TJ, … Jena JK (2022) Usage pattern of chemicals, biologicals and veterinary medicinal products in Indian aquaculture. Reviews in Aquaculture 14(4): 2038–2063.

Rigos G, Kogiannou D (2023) Antimicrobial drugs in aquaculture: use and abuse. In: Knowles ME, Anelich LE, Boobis AR, Popping B (Eds) Present knowledge in food safety - a risk-based approach through the food chain. Academic Press, Cambridge, pp 142–161.

Roberts RJ (2012) Fish Pathology, fourth ed. Blackwell Publishing Ltd, Oxford.

Sadiqul IM, Kabir SM, Ferdous Z, Mansura KM, Khalilur RM (2017) Chronic exposure to quinalphos shows biochemical changes and genotoxicity in erythrocytes of silver barb, *Barbonymus gonionotus*. Interdisciplinary Toxicology 10(3): 99–106.

Sawhney AK, Johal MS (2000) Erythrocyte alterations induced by malathion in *Channa punctatus* (Bloch). Bulletin of Environmental Contamination and Toxicology 64(3): 398–405.

Schar D, Klein EY, Laxminarayan R, Gilbert M, Van Boeckel TP (2020) Global trends in antimicrobial use in aquaculture. Scientific Report 10(1): 21878.

Sehonova P, Tokanova N, Hodkovicova N, Kroupova HK, Tumova J, … Faggio C (2019) Oxidative stress induced by fluoroquinolone enrofloxacin in zebrafish (*Danio rerio*) can be ameliorated after a prolonged exposure. Environmental Toxicology and Pharmacology 67: 87–93.

Shahjahan M, Rahman MS, Islam SM, Uddin MH, Al-Emran M (2019) Increase in water temperature increases acute toxicity of sumithion causing nuclear and cellular abnormalities in peripheral erythrocytes

of zebrafish *Danio rerio*. Environmental Science and Pollution Research 26: 36903–36912.

Shi F, Yao M, Huang Y, Chen Z, Xiao J, … Qin Z (2023) Effects of antibiotics on immunity and apoptosis on grass carp liver and hepatocytes. Journal of Environmental Chemical Engineering 11(3): 110168.

Shin S, Ku Y, Babu N, Singh M (2007) Erythrocyte deformability and its variation in diabetes mellitus. Indian Journal of Experimental Biology 45(1): 121–128.

Stoltz JF, Singh M, Riha P (1999) Hemorheology in Practice (Vol. 30). IOS Press, Amsterdam.

Tomova ES, Velcheva IG, Arnaudov AD (2009) Influence of copper and zinc on the erythrocyte-metric parameters of *Carassius gibelio* (Pisces, Cyprinidae). Bulgarian Journal of Agricultural Science 15(3): 183–188.

Uzunova E (2002) Erythrocyte measurements as a possible approach for distinguishing diploid and triploid brook trout (*Salvelinus fontinalis*, Mitchill, 1814). Acta Zoologica Bulgarica 54(1): 79–86.

Vieira JE, de Oliveira Ferreira R, dos Reis Sampaio DM, da Costa Araújo AP, Malafaia G (2019) An insight on the mutagenicity and cytotoxicity of zinc oxide nanoparticles in *Gallus gallus domesticus* (Phasianidae). Chemosphere 231: 10–19.

Wang N, Noemie N, Hien NN, Huynh TT, Silvestre F, … Huong D (2009) Adverse effects of enrofloxacin when associated with environmental stress in Tra catfish (*Pangasianodon hypophthalmus*). Chemosphere 77(11): 1577–1584.

Witeska M, Kondera E, Bojarski B (2023) Hematological and hematopoietic analysis in fish toxicology - a review. Animals 13(16): 2625.

Zhelev Z, Popgeorgiev G, Ivanov I, Boyadzhiev P (2017) Changes of erythrocyte-metric parameters in *Pelophylax ridibundus* (Amphibia: Anura: Ranidae) inhabiting water bodies with different types of anthropogenic pollution in Southern Bulgaria. Environmental Science and Pollution Research 24(21): 17920–17934.

R Das https://orcid.org/0000-0002-6414-7840
TJ Abraham https://orcid.org/0000-0003-0581-1307
A Sen https://orcid.org/0000-0001-8991-7875
PK Patil https://orcid.org/0000-0002-1924-5863